*Original Article*
*Bulletin of Pure and Applied Sciences.*
*Mathematics & Statistics Vol.45 E, No.2.*
*July-December 2026: P.8-27*

*Print version ISSN 0970 6577*
*Online version ISSN 2320 3226*
*Available online at www.bpasjournals.com*

# Dynamics and Stability Analysis of COVID-19 Using SEAIHR Epidemic Model with Sensitivity and Numerical Investigation

**[1]Raju Kumar*, [2]Dr. P.K. Choudhary**

**Author Affiliation:**
[1]Research Scholar, Department of Mathematics, Patna University, Patna, Bihar, 800005, India
E-mail-rajukumar-rsmaths@pup.ac.in
[2]Associate Professor, Department of Mathematics, Patna University, Patna, Bihar, 800005, India

***Corresponding Author: Raju Kumar**, Department of Mathematics, Patna University, Patna, Bihar, 800005, India
E-mail: rajukumar-rsmaths@pup.ac.in

**ABSTRACT**
This study develops and analyzes a modified SEAIHR (Susceptible–Exposed–Asymptomatic–Infectious–Hospitalized–Recovered) epidemic model to investigate the transmission dynamics of COVID-19 in India. The model incorporates awareness, self-monitoring, and hospitalization effects to reflect behavioral adaptation and clinical transitions within the population. Mathematical properties such as positivity, boundedness, and the existence of equilibrium points are established to ensure biological feasibility. The basic reproduction number, derived using the next-generation matrix approach, is obtained as $R_o$=2.5307 , indicating that the infection can persist under baseline conditions. Local and global stability analyses are performed for both disease-free and endemic equilibria using the Routh–Hurwitz and Lyapunov methods. Sensitivity (elasticity) analysis of $R_o$ reveals that the transmission coefficient ($\alpha$) the progression fraction to symptomatic infection ($\theta_i$) , and the infectiousness coefficient of symptomatic individuals ($e_2$) are the most influential parameters enhancing disease spread. In contrast, removal and hospitalization rates $(d_r, d_h, \beta)$ exhibit negative elasticities, signifying their effectiveness in disease control. Numerical simulations based on the classical fourth-order Runge–Kutta (RK4) method with a fixed time step of $\Delta t = 0.1$ day validate the analytical findings. The time-series trajectories show typical epidemic peaks with convergence to a stable endemic equilibrium for $R_0$>1 , while phase-plane plots confirm global asymptotic stability. The results emphasize that early detection, isolation, and improved hospitalization efficiency can substantially mitigate COVID-19 transmission and ensure long-term disease control in India.

**Keywords:** COVID-19; SEAIHR model, Stability analysis, Sensitivity analysis

**How to cite this article:** Kumar R., Choudhary P.K. Dynamics and Stability Analysis of COVID-19 Using SEAIHR Epidemic Model with Sensitivity and Numerical Investigation. *Bulletin of Pure and Applied Sciences- Math & Stat.*, 2026;45E (1):8-27.

**Received on 25.04.2026, Revised on 20.06.2026, Accepted on 19.07.2026**

## 1. INTRODUCTION

The COVID-19 pandemic has motivated extensive mathematical modelling to understand transmission mechanisms and to evaluate public-health interventions. Classical compartmental models (SIR/SEIR) provide transparent frameworks for epidemic thresholds, control design and forecasting, but the complex clinical progression and behavioral responses associated with SARS-CoV-2 require extended formulations that explicitly account for asymptomatic infection, hospitalization and awareness-driven changes in contact patterns [1–4]. Recent comparative studies emphasize that behavioral feedbacks and healthcare compartments materially alter epidemic trajectories and policy recommendations, particularly in high-density settings such as India [5–8].

In India, a number of SEIR-type and multi-compartment studies have sought to capture the timing and magnitude of epidemic waves, projections of hospital demand, and the effects of non-pharmaceutical interventions (NPIs). These works demonstrate that region-specific demography, under-reporting, and delayed hospitalization can substantially affect peak incidence and healthcare burden [9–12]. At the same time, models that omit explicit hospitalization or awareness mechanisms risk under-estimating the mitigating impact of timely detection, isolation and hospital care [11,13]. From a theoretical perspective, rigorous derivation of the basic reproduction number $R_0$ via the next-generation matrix and proofs of

local and global stability are essential for establishing thresholds for disease control [12,14]. Complementary sensitivity and elasticity analyses identify which parameters most strongly influence $R_0$

and therefore represent priority targets for intervention; the normalized forward sensitivity (elasticity) approach and variance-based global methods are now standard in epidemic modelling [15–17]. Numerical integration (RK4 or high-accuracy ODE solvers) is used to validate analytic claims and to produce time-series and phase-plane diagnostics for scenario analysis [3,18].

Motivated by these considerations, we propose a modified SEAIHR model that partitions infectious individuals into asymptomatic, symptomatic and hospitalized classes and incorporates an awareness/self-monitoring mechanism that reduces effective transmission as cases and hospitalizations grow. This explicit representation allows direct study of how detection, removal and hospitalization policies shape both transient peaks and long-term endemic behavior. Methodologically, we derive $R_0$ in

closed form, establish positivity and boundedness, and prove local and global stability of the disease-free and endemic equilibria using Routh–Hurwitz and Lyapunov techniques. We then compute normalized sensitivity indices of $R_0$ to rank influential parameters and perform India-scale numerical simulations (RK4, $\Delta t = 0.01$ day) to illustrate time-series and phase-plane behavior under baseline and perturbed scenarios. Our approach follows and extends prior modeling efforts that account for awareness and hospitalization in COVID-19 dynamics [10,12,19–22].

The principal contributions of this study are: (i) formulation and rigorous analysis of an SEAIHR model that integrates awareness and hospitalization effects; (ii) derivation of a closed-form $R_0$ and proof of stability properties; (iii) an elasticity-based sensitivity ranking that highlights optimal control levers; and (iv) India-scale numerical simulations demonstrating the timing and magnitude of epidemic peaks and hospital burden. These results aim to inform policy on testing, isolation, and hospital preparedness in contexts with similar demographic and healthcare constraints.

## 2. MODEL FORMULATION

Mathematical modeling has been widely used to understand and predict the dynamics of infectious diseases, including COVID-19. Compartmental models, such as SIR, SEIR, and their extensions, provide insights into the transmission dynamics and effectiveness of control strategies [23–25]. For COVID-19, several studies have extended the classical SEIR framework to incorporate asymptomatic infections, hospitalization, and recovery compartments, recognizing the role of asymptomatic carriers in disease propagation [26–28].

Recent studies have applied SEAIHR-type models for COVID-19. For example, Saha et al. [29] used an SEQAIHR model to study transmission dynamics with treatment saturation. Zong et al. [30] highlighted the importance of age-specific interventions using a multigroup SEAIHRD model. Stability and sensitivity analyses of SEAIHR models provide insights into control strategies and the impact of interventions such as vaccination and mask usage [31,32]. Numerical simulations validate the model predictions and help understand disease progression over time [33].

In this study, the entire population $(\mathbf{N})$ is partitioned into six distinct compartments: susceptible $\mathbf{S}$, exposed $\mathbf{E}$, asymptomatic $\mathbf{A}$, symptomatic infected $\mathbf{I}$, hospitalized $\mathbf{H}$, and recovered $\mathbf{R}$. The SEAIHR model is adopted for COVID-19 in India, incorporating asymptomatic transmission, hospitalization, and recovery processes, providing a robust framework for analyzing disease dynamics and intervention strategies.

Thus,

$$N(t) = S(t) + E(t) + A(t) + I(t) + H(t) + R(t)$$

**Susceptible S(t)**

**Compartment S(t)** contains individuals who are at risk of contracting the infection. It increases through recruitment at a constant rate $\Lambda_s$. Susceptible individuals leave this class when they come into effective contact with infectious individuals in the asymptomatic, symptomatic, or hospitalized compartments, weighted by their relative infectiousness coefficients and governed by the transmission rate $\alpha$. Natural deaths also reduce the number of susceptible at rate $\eta$. These combined effects yield the governing equation

$$\frac{dS}{dt} = \Lambda_s - \frac{\alpha S}{N}(e_1 A + e_2 I + e_3 H) - \eta S$$

**Exposed $(E)$**

The exposed compartment consists of individuals who have been infected but are not yet infectious. They enter this class after contact with infectious persons and leave either by progressing to the infectious stage at rate $\delta$, by being removed through self-monitoring or isolation at rate $d_e$, or by dying naturally at rate $\eta$. Therefore, the governing equation for this group is

$$\frac{dE}{dt} = \frac{\alpha S}{N}(e_1 A + e_2 I + e_3 H) - (\delta + d_e + \eta)E$$

**Asymptomatic infectious ($A$)**

A fraction $\sigma_a$ of exposed individuals becomes asymptomatic infectious. These individuals can transmit the disease but do not show symptoms. They recover at rate $\gamma$, can be removed due to self-monitoring at rate $d_a$, and also experience natural mortality at rate $\eta$ . Therefore, the governing equation for this group is

$$\frac{dA}{dt} = \sigma_a \delta E - (\gamma + d_a + \eta)A$$

**Symptomatic infectious ($I$)**

A fraction $\sigma_i$ of exposed individuals develops symptoms and enters the symptomatic infectious class. These individuals may progress to hospitalization at rate $\beta$, may be removed due to self-monitoring at rate $d_i$, or die naturally at rate $\eta$. These combined processes are expressed by the governing equation.

$$\frac{dI}{dt} = \sigma_i \delta E - (\beta + d_i + \eta)I$$

**Hospitalized ($H$)**

Hospitalized individuals come from the symptomatic class at rate $\beta$. They can recover from the disease at rate $\mu$, may be removed through self-monitoring at rate $d_h$, or die naturally at rate $\eta$. Therefore, the governing equation for this group

$$\frac{dH}{dt} = \beta I - (\mu + d_h + \eta)H$$

**Recovered ($R$)**

The recovered class consists of individuals who gained immunity after infection. It increases as asymptomatic individuals recover at rate $\gamma$ and hospitalized individuals recover at rate $\mu$. Natural mortality reduces this class at rate $\eta$, and recovered individuals are assumed to have permanent immunity. The resulting dynamics of the recovered population are governed by

$$\frac{dR}{dt} = \gamma A + \mu H - \eta R$$

The dynamics of the COVID-19 epidemic model are determined by the following system of nonlinear ordinary differential equations:

$$\begin{cases} \frac{dS}{dt} = \Lambda_s - \frac{\alpha S}{N}(e_1 A + e_2 I + e_3 H) - \eta S \\ \frac{dE}{dt} = \frac{\alpha S}{N}(e_1 A + e_2 I + e_3 H) - (\delta + d_e + \eta)E \\ \frac{dA}{dt} = \sigma_a \delta E - (\gamma + d_a + \eta)A \\ \frac{dI}{dt} = \sigma_i \delta E - (\beta + d_i + \eta)I \\ \frac{dH}{dt} = \beta I - (\mu + d_h + \eta)H \\ \frac{dR}{dt} = \gamma A + \mu H - \eta R \end{cases} \quad \ldots\ldots\ldots (1)$$

Corresponding initial condition are:

$$S(0) = S_0 \geq 0, E(0) = E_0 \geq 0, A(0) = A_0 \geq 0, I(0) = I_0 \geq 0, H(0) = H_0 \geq 0, R(0) = R_0 \geq 0$$

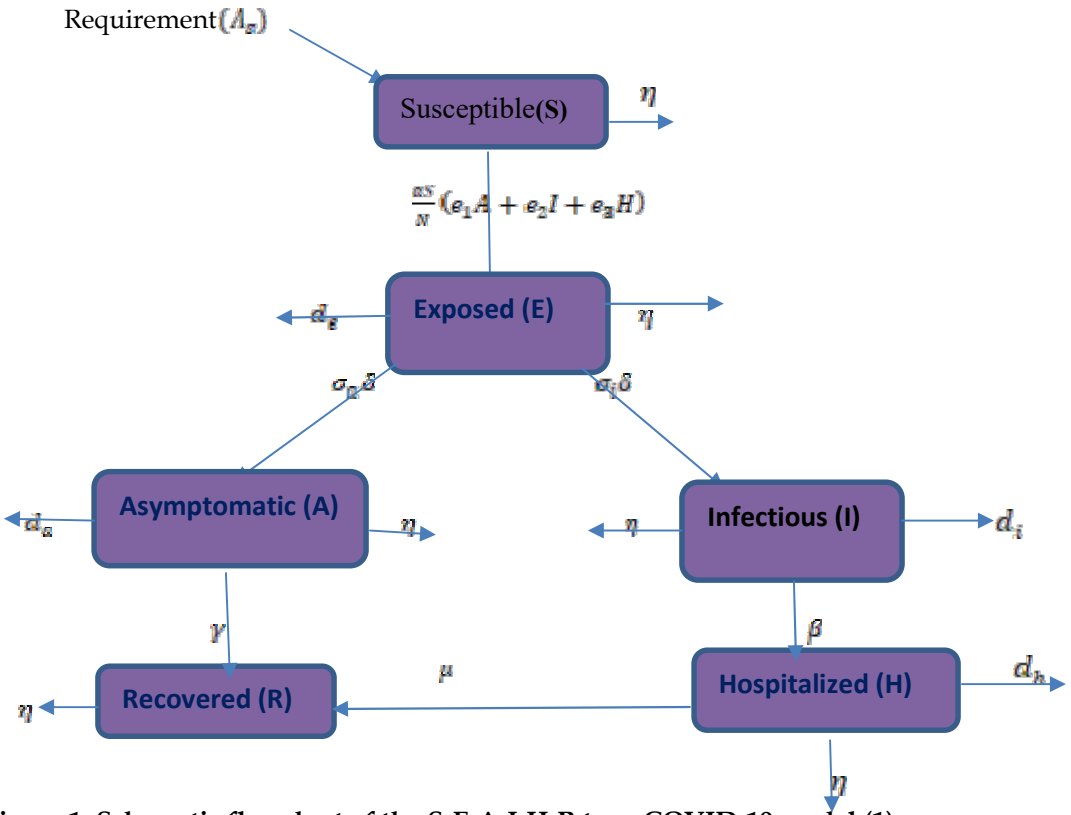


**Figure 1: Schematic flowchart of the S-E-A-I-H-R type COVID-19 model (1).**

**Table 1: Parameter Description and Values**

| Symbol | Description | Value(per day) | Sources |
|---|---|---|---|
| $\Lambda_s$ | Recruitment / net inflow of susceptible | 700 | [34] |
| $\eta$ | Natural death rate | 0.003589 | [37] |
| $\alpha$ | Transmission coefficient | 1.8 | [34] |
| $e_1$ | Self-protection/infectiousness coefficient (A) | 0.3239 | Awareness effect, India; [36] |
| $e_2$ | Self-protection/infectiousness coefficient (I) | 0.9175 | Indian behavioral response; [36], [37] |
| $e_3$ | Self-protection/infectiousness coefficient (H) | 0.5316 | Hospital isolation efficiency; [36] |
| $\delta$ | Progression rate from exposed to infectious | $1/6 \approx 0.1667$ | Incubation period from India data; [35], [38] |
| $d_e$ | Auto-monitoring / removal rate in $E$ | 0.1753 | Public awareness; [38], [34] |
| $\sigma_a$ | Fraction E → asymptomatic A | 0.13166 | Estimated for Indian cases; [38] |
| $\sigma_i$ | Fraction E → asymptomatic I | 0.86834 | Indian epidemic data; [38] |
| $\gamma$ | Recovery rate of asymptomatic A | 0.2 | Average 5 days recovery; [35], [36] |
| $d_a$ | Auto-monitoring / removal rate in $A$ | 0.1741 | Asymptomatic testing; [38], [34] |

| | | | |
|---|---|---|---|
| $\beta$ | Rate of symptomatic I→H | 0.2042 | Indian COVID-19 wave; [38] |
| $d_i$ | Auto-monitoring / removal rate in $I$ | 0.1742 | Case tracking; [38], [34] |
| $\mu$ | Recovery rate of hospitalized | $1/6 \approx 0.16667$ | Clinical data from Indian hospitals; [37] |
| $d_h$ | Auto-monitoring / removal rate in $H$ | 0.1742 | Hospital safety protocols; [38], [34] |

## 3. SEAIHR MODEL ANALYSIS

### 3.1 Positivity of the solutions

For the model (1) to be epidemiologically meaningful and Mathematically well poised, it is necessary to prove that all state variables remain nonnegative $\forall\, t \geq 0$.

**Theorem 1:**

Let $\{S(0) = S_0 \geq 0,\ E(0) = E_0 \geq 0,\ A(0) = A_0 \geq 0,\ I(0) = I_0 \geq 0,\ H(0) = H_0 \geq 0,\ R(0) = R_0 \geq 0\} \in R_+^6$

Then the solutions $\{S(t),\ E(t),\ A(t),\ I(t),\ H(t),\ R(t)\}$ of the model system (1) are positive for all $t \geq 0$

Proof: To prove this theorem, we used the approach in [39], where we take into account system of model (1). Consider the first equation from model (1),

$$\frac{dS}{dt} = \Lambda_s - \frac{\alpha S}{N}(e_1 A + e_2 I + e_3 H) - \eta S$$

$$\frac{dS}{dt} \geq -\left(\frac{\alpha}{N}(e_1 A + e_2 I + e_3 H) + \eta\right) S \geq -(\alpha(e_1 + e_2 + e_3) + \eta) S$$

$$\frac{dS}{dt} \geq -(\alpha(e_1 + e_2 + e_3) + \eta) S \qquad \ldots\ (3.1.1)$$

Apply variable separable technique in Eq. (3.1.1) and introduce limit from 0 to $t$ results

$$\int_{S(0)}^{S(t)} \frac{dS}{S} \geq -\int (\alpha(e_1 + e_2 + e_3) + \eta)\, dt$$

Further simplification leads to:

$S(t) \geq S_0 e^{-(\alpha(e_1+e_2+e_3)+\eta)t}$, which implies

$S(t) \geq 0$

Consider the second equation from model (1),

$$\frac{dE}{dt} = \frac{\alpha S}{N}(e_1 A + e_2 I + e_3 H) - (\delta + d_e + \eta) E$$

$$\frac{dE}{dt} \geq -(\delta + d_e + \eta) E, \qquad \ldots\ (3.1.2)$$

Apply variable separable technique in Eq. (3.1.2) and introduce limit from 0 to $t$ results

$$\int_{E(0)}^{E(t)} \frac{dE}{E} \geq -\int (\delta + d_e + \eta)\, dt$$

Further simplification leads to:

$E(t) \geq E_0 e^{-(\delta + d_e + \eta)t}$, Which implies

$E(t) \geq 0$

This shows that the solution for susceptible $S(t)$ and exposed $E(t)$ population is non negative$\forall t \geq 0$. Doing the same approach to the remaining equations in the model (1), it can be simply shown that

$A(t) \geq 0,\ I(t) \geq 0,\ H(t) \geq 0,\ I(t) \geq 0,\ R(t) \geq 0$ for all $t \geq 0$ Therefore $(S(t),\ E(t),\ A(t),\ I(t),\ H(t),\ R(t))$ of the model Eq.(1) is nonnegative $\forall t \geq 0$.This completes the proof of Theorem1 □

### 3.2. Boundedness and Invariant Region

The invariant region specifies the set in which the solutions of model (1) are valid from both a biological and mathematical perspective. Because all model parameters are assumed to be non-negative for all $t \geq 0$, any solution starting with positive initial conditions will remain non-negative for all future time and will stay bounded within this region.

**Theorem 2:**

The solution set of $S(t),\ E(t),\ A(t),\ I(t),\ H(t),\ R(t)$ of the model Equation system(1) is confined in a positive feasible region Ω

**Proof.** Suppose the feasible region $\Omega = (S(t),\ E(t),\ A(t),\ I(t),\ H(t),\ R(t)) \in R_+^6, \forall t \geq 0$

At any time $t$ the total population $N(t)$will be: $N(t) = S(t) + E(t) + A(t) + I(t) + H(t) + R(t)$

Differentiating with respect to $t$ leads to

$$\frac{dN}{dt} = \frac{dS}{dt} + \frac{dE}{dt} + \frac{dA}{dt} + \frac{dI}{dt} + \frac{dH}{dt} + \frac{dR}{dt} \qquad \ldots (3.2.1)$$

Substitute Eq. (1) into Eq. $(3.2.1)$ further simplification result into,

$$\frac{dN}{dt} = \Lambda_s + (\sigma_a + \sigma_i)\delta E - \delta E - \eta(S + E + A + I + H + R) - (d_e E + d_a A + d_i I + d_h H)$$

Because $(\sigma_a + \sigma_i) = 1$(the exposed individuals either become asymptomatic or symptomatic)

$$\frac{dN}{dt} = \Lambda_s + 1.\delta E - \delta E - \eta(N) - (d_e E + d_a A + d_i I + d_h H)$$

Because the disease-induced removal rates $d_e, d_a, d_i, d_h$ are nonnegative, we have the inequality

$$\frac{dN(t)}{dt} \leq \Lambda_s - \eta N(t)$$

This is a standard linear differential inequality. Apply **Grönwall's inequality** (or solve the linear ODE):

$$N(t) \leq N(0)e^{-\eta t} + \frac{\Lambda_s}{\eta}(1 - e^{-\eta t})$$

Further simplification leads to

Thus,

$\lim_{t\to\infty} sup N(t) \leq \frac{\Lambda}{\eta}$. Finally $\Omega = \left\{(S(t),\ E(t),\ A(t),\ I(t),\ H(t),\ R(t)) \in R_+^6 : 0 < N(t) \leq \frac{\Lambda}{\eta}\right\}\ \forall t \geq 0$

The domain Ω is a positive invariant under the flow induced by the system model (1). Therefore, all feasible solutions of the model (1) enter the region Ω, hence the proposed COVID-19 model system (1) is well-posed and is both epidemiologically and mathematically meaningful and we consider to generate the analysis. This implies that, the model system is positive invariant in the region.

$\Omega = \left\{(S(t),\ E(t),\ A(t),\ I(t),\ H(t),\ R(t)) \in R_+^6 : 0 < N(t) \leq \frac{\Lambda}{\eta}\right\}\ \forall t \geq 0$

For $\{S(0) = S_0,\ E(0) = E_0,\ A(0) = A_0,\ I(0) = I_0,\ H(0) = H_0,\ R(0) = R_0\} \geq 0 \in \Omega$ and this completes the proof. □

### 3.3. Disease free equilibrium point (DFE)

At DFE there is no infection: $E = A = I = H = R = 0$. Solve steady state for susceptible and recovered:

From $\frac{dS}{dt} = 0$ with no infection we get $\Lambda_s - \eta S^0 = 0$ so $S^0 = \frac{\Lambda_s}{\eta}$

From $\frac{dR}{dt} = 0$ and $A^0 = H^0 = 0$ we get $0 - \eta R^0 = 0 \Rightarrow R^0 = 0$. Total $N^0 = S^0 = \frac{\Lambda_s}{\eta}$.

Thus the DFE is

$$E_0 = (S^0, E^0, A^0, I^0, H^0, R^0) = \left(\frac{\Lambda_s}{\eta}, 0, 0, 0, 0, 0\right).$$

### 3.4. Basic Reproduction Number

The basic reproduction number $(R_0)$ is an important epidemiological threshold parameter that determines whether an infectious disease can invade and persist in a population. It can be computed using the next-generation operator approach, following the method of van den Driessche and Watmough (2002) [40].

From the model system (1) the infected compartments are

$$\begin{cases} \frac{dE}{dt} = \frac{\alpha S}{N}(e_1 A + e_2 I + e_3 H) - (\delta + d_e + \eta)E \\ \frac{dA}{dt} = \sigma_a \delta E - (\gamma + d_a + \eta)A \\ \frac{dI}{dt} = \sigma_i \delta E - (\beta + d_i + \eta)I \\ \frac{dH}{dt} = \beta I - (\mu + d_h + \eta)H \end{cases} \quad \ldots\ldots\ldots \quad (3.4.1)$$

Now, from (3.4.1) $F_i$ (new infection terms) and $V_i$ (transition terms) are given as follows

$$F_i = \begin{bmatrix} F_1 \\ F_2 \\ F_3 \\ F_4 \end{bmatrix} = \begin{bmatrix} \frac{\alpha S}{N}(e_1 A + e_2 I + e_3 H) \\ 0 \\ 0 \\ 0 \end{bmatrix}$$

$$V_i = \begin{bmatrix} V_1 \\ V_2 \\ V_3 \\ V_4 \end{bmatrix} = \begin{bmatrix} (\delta + d_e + \eta)E \\ (\gamma + d_a + \eta)A - \sigma_a \delta E \\ (\beta + d_i + \eta)I - \sigma_i \delta E \\ (\mu + d_h + \eta)H - \beta I \end{bmatrix}$$

Then, by differentiating $F$ and $V$ partially with respect to $E, A, I$ and $H$ at disease free equilibrium point we get,

$$= \left(\frac{\partial F_i}{\partial (E, A, I, H)}\right)_{\varepsilon_0} = \begin{bmatrix} 0 & \alpha e_1 & \alpha e_2 & \alpha e_3 \\ 0 & 0 & 0 & 0 \\ 0 & 0 & 0 & 0 \\ 0 & 0 & 0 & 0 \end{bmatrix}$$

$$V = \left(\frac{\partial V_i}{\partial (E, A, I, H)}\right)_{\varepsilon_0} = \begin{bmatrix} (\delta + d_e + \eta) & 0 & 0 & 0 \\ -\sigma_a \delta & (\gamma + d_a + \eta) & 0 & 0 \\ -\sigma_i \delta & 0 & (\beta + d_i + \eta) & 0 \\ 0 & 0 & -\beta & (\mu + d_h + \eta) \end{bmatrix}$$

Now, the next generation matrix is:

$$K = FV^{-1}$$

Because $F$ has only the first row nonzero, $K$ is a rank-1 matrix. Its spectral radius (largest eigenvalue) is simply the first row of $F$ times the first column of $V^{-1}$.

So,

$$R_0 = \alpha\left[e_1\frac{\sigma_a\delta}{(\delta+d_e+\eta)(\gamma+d_a+\eta)} + e_2\frac{\sigma_i\delta}{(\delta+d_e+\eta)(\beta+d_i+\eta)} + e_3\frac{\sigma_i\delta\beta}{(\delta+d_e+\eta)(\beta+d_i+\eta)(\mu+d_h+\eta)}\right]$$

**3.5 Stability analysis of DFE**

**Theorem 3:**

The DFE $E_0$, is locally asymptotically stable if $R_0 < 1$ and otherwise unstable.

Proof. The Jacobian matrix corresponding to the system (1) at DFE $E_0$, is

$$J(E_0) = \begin{bmatrix} -\eta & 0 & -\alpha e_1 & -\alpha e_1 & -\alpha e_2 & 0 \\ 0 & -(\delta+d_e+\eta) & -\alpha e_1 & -\alpha e_2 & -\alpha e_3 & 0 \\ 0 & \sigma_a\delta & -(\gamma+d_a+\eta) & 0 & 0 & 0 \\ 0 & \sigma_i\delta & 0 & -(\beta+d_i+\eta) & 0 & 0 \\ 0 & 0 & 0 & \beta & -(\mu+d_h+\eta) & 0 \\ 0 & 0 & \gamma & 0 & \mu & -\eta \end{bmatrix}$$

Eigenvalues corresponding to non-infectious compartments

From the Jacobian, it is clear that three eigenvalues are directly visible:

$-\eta, -\eta$ and These are all negative since parameters are positive.

The dynamics of infection are determined by the submatrix of infected compartments $(E, A, I, H)$ :

$$J_{infected} = \begin{bmatrix} -(\delta+d_e+\eta) & -\alpha e_1 & -\alpha e_2 & -\alpha e_3 \\ \sigma_a\delta & -(\gamma+d_a+\eta) & 0 & 0 \\ \sigma_i\delta & 0 & -(\beta+d_i+\eta) & 0 \\ 0 & 0 & \beta & -(\mu+d_h+\eta) \end{bmatrix}$$

For simplicity, define

$a = (\delta+d_e+\eta),\ b = (\gamma+d_a+\eta),\ c = (\beta+d_i+\eta),\ d = (\mu+d_h+\eta)$

So that $a > 0, b > 0, c > 0, d > 0$

The characteristic polynomial of $J_{infected}$ is

$ch(\lambda) = \det(J_{inf} - \lambda I) = \lambda^4 + A_1\lambda^3 + A_2\lambda^2 + A_3\lambda + A_4$

With

$$A_1 = a+b+c+d, A_2 = ab+ac+ad+bc+bd+cd-\alpha\delta(\sigma_a e_1+\sigma_i e_2)$$

$$A_3 = abc+abd+acd+bcd-\alpha\delta(b\sigma_i e_2+\beta\sigma_i e_3+c\sigma_a e_1+d\sigma_a e_1+d\sigma_i e_2)$$

$$A_4 = abcd(1-R_0),$$

where the basic reproduction number, $R_0 = \alpha\left(\frac{e_1\sigma_a\delta}{ab}+\frac{e_2\sigma_i\delta}{ac}+\frac{e_3\sigma_i\delta\beta}{acd}\right)$

Here $-\eta, -\eta$ are the first two eigenvalue of $J(E_*)$ and the remaining four eigenvalues will be attained from the fourth degree equation $(\lambda^4 + A_1\lambda^3 + A_2\lambda^2 + A_3\lambda + A_4) = 0$

According to the Routh–Hurwitz stability criterion [40-42] DFE $(E_0)$ is locally asymptotically stable if the following condition are satisfied:

$(i).\ A_1 > 0, A_2 > 0, A_3 > 0, A_4 > 0,$

$(ii).\ A_1A_2 > A_3$

$(iii).\ A_1A_2A_3 > A_1^2A_4 + A_3^2.$

Cleary $A_1 > 0, A_2 > 0, A_3 > 0$, the sign of the constant term is governed by the factor $(1-R_0)$. Thus,

$$A_4 > 0 \Leftrightarrow R_0 < 1$$

Therefore, when $R_0 < 1$ all Routh–Hurwitz conditions are satisfied, and the DFE is locally asymptotically stable. Conversely, if $R_0 > 1$, then $A_4 < 0$, which violates the criterion, and hence the DFE is unstable.

**Theorem 4:**
The disease-free equilibrium( $E_0$) of the model system (1) is globally asymptotically stable if $R_0 < 1$ .
**Proof.** To prove theorem 4. the method used by Liaoand Wang [43] is applied. Then, it is required to show that the conditions($H_1$) and($H_2$) hold if $R_0 < 1$

The model system can be written in form of $X = (S, R), Y = (E, A, I, H)$ and

$$(E_0) = (X^0, 0) = \left(\frac{\Lambda_s}{\eta}, 0, 0, 0, 0, 0\right)$$

Then,

$$\frac{dX}{dt} = \begin{pmatrix} \Lambda_s - \frac{\alpha S}{N}(e_1 A + e_2 I + e_3 H) - \eta S \\ \gamma A + \mu H - \eta R \end{pmatrix}$$

At DFE $(E_0) = (X^0, 0)$ gives,

$$\frac{dX}{dt} = F(X, 0) = \begin{pmatrix} \Lambda_s - \eta S \\ -\eta R \end{pmatrix} \quad \ldots (4.1)$$

The first row of the matrix from (4.1) can be written as, $\frac{dS(t)}{dt} = \Lambda_s - \eta S$

This is linear first ODEs and its solution can be found as:

$$S(t) = \frac{\Lambda_s}{\eta} + \left(S(0) - \frac{\Lambda_s}{\eta}\right) e^{-\eta t} \quad \ldots\ldots\ldots (4.2)$$

Again, the second row from the matrix can be written as

$$\frac{dR(t)}{dt} = -\eta R$$

This is linear first ODEs and its solution can be found as:

$$R(t) = R(0) e^{-\eta t} \quad \ldots\ldots (4.3)$$

Hence from $S(t)$ and $R(t)$, it is clearly that, $S(t) \to \frac{\Lambda_s}{\eta}, R(t) \to 0 \text{ as } t \to \infty$

Thus $X^*$ is globally asymptotically stable for $\frac{dX}{dt} = F(X, 0)$.

Therefore, the first condition ($H_1$) is satisfied.
For condition ($H_2$) we have

$$G(X, Y) = \begin{pmatrix} \frac{\alpha S}{N}(e_1 A + e_2 I + e_3 H) - (\delta + d_e + \eta) E \\ \sigma_a \delta E - (\gamma + d_a + \eta) A \\ \sigma_i \delta E - (\beta + d_i + \eta) I \\ \beta I - (\mu + d_h + \eta) H \end{pmatrix}$$

Then, it gives,

$$\frac{\partial G(X, Y)}{\partial Y} = \begin{pmatrix} -(\delta + d_e + \eta) & \alpha e_1 & \alpha e_2 & \alpha e_3 \\ \sigma_a \delta & -(\gamma + d_a + \eta) & 0 & 0 \\ \sigma_i \delta & 0 & -(\beta + d_i + \eta) & 0 \\ 0 & 0 & \beta & -(\mu + d_h + \eta) \end{pmatrix}$$

Where $Y = (E, A, I, H)$. Since, it is clearly the Matrix $A = D_Y G(X^0, 0)$ is a Metzler matrix (its off diagonal elements are nonnegative. Then, $\bar{G}(X, Y) = AY - G(X, Y)$

That is,

$$\bar{G}(X,Y)=\begin{pmatrix}-(\delta+d_e+\eta) & \alpha e_1 & \alpha e_2 & \alpha e_3\\ \sigma_\alpha\delta & -(\gamma+d_\alpha+\eta) & 0 & 0\\ \sigma_i\delta & 0 & -(\beta+d_i+\eta) & 0\\ 0 & 0 & \beta & -(\mu+d_h+\eta)\end{pmatrix}\begin{pmatrix}E\\A\\I\\H\end{pmatrix}$$

$$-\begin{pmatrix}\frac{\alpha S}{N}(e_1A+e_2I+e_3H)-(\delta+d_e+\eta)E\\ \sigma_\alpha\delta E-(\gamma+d_\alpha+\eta)A\\ \sigma_i\delta E-(\beta+d_i+\eta)I\\ \beta I-(\mu+d_h+\eta)H\end{pmatrix}$$

$$\bar{G}(X,Y)=\begin{pmatrix}\alpha(Ae_1+Ie_2+He_3)-\frac{\alpha S}{N}(Ae_1+Ie_2+He_3)\\ 0\\ 0\\ 0\end{pmatrix}$$

Since, $\alpha(Ae_1+Ie_2+He_3)>\frac{\alpha S}{N}(Ae_1+Ie_2+He_3)$ it is clear that $\bar{G}(X,Y)\geq 0$

Thus the second condition $(H_2)$ also satisfied.

Hence the disease-free equilibrium $(E_0)$ is globally asymptotically stable in the region $\Omega$ for $R_0<1$.

**3.5. Endemic Equilibrium**

To find the endemic equilibrium, we set the time derivatives in the model (1) to zero. This gives a system of algebraic equations:

$\Lambda_s-\frac{\alpha S^*}{N^*}(e_1A^*+e_2I^*+e_3H^*)-\eta S^*=0$ ……. [3.5.1]

$\frac{\alpha S^*}{N^*}(e_1A^*+e_2I^*+e_3H^*)-(\delta+d_e+\eta)E^*=0$ ….. [3.5.2]

$\sigma_\alpha\delta E^*-(\gamma+d_\alpha+\eta)A^*=0$ ……. [3.5.3]

$\sigma_i\delta E^*-(\beta+d_i+\eta)I^*=0$ ……. [3.4.4]

$\beta I^*-(\mu+d_h+\eta)H^*=0$ …… [3.5.5]

$\gamma A^*+\mu H^*-\eta R^*=0$ …. [3.5.6]

Let, $a=(\delta+d_e+\eta),\ b=(\gamma+d_\alpha+\eta),\ c=(\beta+d_i+\eta),\ d=(\mu+d_h+\eta)$

And $\lambda^*=\frac{\alpha S^*}{N^*}(e_1A^*+e_2I^*+e_3H^*)$

Then from equation [3.5.2] we get.

$$E^*=\frac{\lambda^*}{a}$$

Then from equation [3.5.3] we get

$$A^*=\frac{\sigma_\alpha\delta E^*}{b}=\frac{\sigma_\alpha\delta\lambda^*}{ab}$$

Then from equation [3.5.4] we get

$$I^*=\frac{\sigma_i\delta E^*}{c}=\frac{\sigma_i\delta\lambda^*}{ac}$$

Then from equation [3.5.5] we get

$$H^*=\frac{\beta I^*}{d}=\frac{\beta\sigma_i\delta\lambda^*}{acd}$$

Then from equation [3.5.6] we get

$$R^*=\frac{\gamma A^*+\mu H^*}{\eta}=\frac{1}{\eta}\left(\frac{\gamma\sigma_\alpha\delta}{ab}+\frac{\mu\beta\sigma_i\delta}{acd}\right)\lambda^*$$

Now $\lambda^* = \frac{\alpha S^*}{N^*}(e_1 A^* + e_2 I^* + e_3 H^*) = \frac{\alpha S^*}{N^*}\left(\frac{e_1\sigma_a\delta}{\alpha b} + \frac{e_2\sigma_i\delta}{\alpha c} + \frac{e_3\sigma_i\delta\beta}{\alpha c d}\right)\lambda^* = \frac{S^*}{N^*}R_0\lambda^*$

$\lambda^* = \frac{S^*}{N^*}R_0\lambda^* \Rightarrow \frac{1}{R_0} = \frac{S^*}{N^*}$

Total population at equilibrium:

$N^* = S^* + (E^* + A^* + I^* + H^* + R^*)$

$$= S^* + \left(\frac{1}{\alpha} + \frac{\sigma_a\delta}{\alpha b} + \frac{\sigma_i\delta}{\alpha c} + \frac{\beta\sigma_i\delta}{\alpha c d} + \frac{1}{\eta}\left(\frac{\gamma\sigma_a\delta}{\alpha b} + \frac{\mu\beta\sigma_i\delta}{\alpha c d}\right)\right)\lambda^*$$

$\Rightarrow \quad N^* = \frac{N^*}{R_0} + C\lambda^* \quad \Rightarrow \quad N^* = \frac{CR_0}{(R_0-1)}\lambda^*$ valid for $(R_0 > 1)$

Thus, the endemic equilibrium $E_*$ is given by

$$S^* = \frac{N^*}{R_0} = \frac{C\lambda^*}{(R_0-1)}, E^* = \frac{\lambda^*}{\alpha}, A^* = \frac{\sigma_a\delta\lambda^*}{\alpha b}, I^* = \frac{\sigma_i\delta\lambda^*}{\alpha c}, H^* = \frac{\beta\sigma_i\delta\lambda^*}{\alpha c d}, R^* = \frac{1}{\eta}\left(\frac{\gamma\sigma_a\delta}{\alpha b} + \frac{\mu\beta\sigma_i\delta}{\alpha c d}\right)\lambda^*$$

3.6. Local stability of the endemic equilibrium

To examine the stability of the endemic equilibrium, we linearize the model around $E_* = (S^*, R^*, E^*, A^*, I^*, H^*)$ and obtain the Jacobian matrix, $J(E_*)$

$$J(S^*R^*, E^*, A^*, I^*, H^*) = \begin{bmatrix} -\frac{\alpha}{N^*}(e_1A^* + e_2I^* + e_3H^*)\left(1 - \frac{S^*}{N^*}\right) - \eta & 0 & 0 & -\frac{\alpha S^* e_1}{N^*} & -\frac{\alpha S^* e_2}{N^*} & -\frac{\alpha S^* e_3}{N^*} \\ 0 & -\eta & 0 & 0 & 0 & \mu \\ \frac{\alpha S^*}{N^*}(e_1A^* + e_2I^* + e_3H^*) & 0 & -(\delta + d_e + \eta) & \frac{\alpha S^* e_1}{N^*} & \frac{\alpha S^* e_2}{N^*} & \frac{\alpha S^* e_3}{N^*} \\ 0 & 0 & \sigma_a\delta & -(\gamma + d_a + \eta) & 0 & 0 \\ 0 & 0 & \sigma_i\delta & 0 & -(\beta + d_i + \eta) & 0 \\ 0 & 0 & 0 & 0 & \beta & -(\mu + d_h + \eta) \end{bmatrix}$$

i.e. put the susceptible–recovered compartments first and the four infected compartments after. Under this ordering the Jacobian evaluated at an equilibrium $(E_*)$ has the **upper block-triangular** form

$$J(E_*) = \begin{bmatrix} J_{SR} & J_{SI} \\ 0 & J_I \end{bmatrix}$$

Hence the characteristic polynomial of $J(E_*)$ factorizes as

$\det(J_{E_*} \quad \lambda I) = \det(J_{SR} \quad \lambda I_2)\det(J_I \quad \lambda I_4)$

S–R block (at the endemic equilibrium $E_*$)

$$J_{SR} = \begin{bmatrix} -\frac{\alpha}{N^*}(e_1A^* + e_2I^* + e_3H^*)\left(1 - \frac{S^*}{N^*}\right) - \eta & 0 \\ 0 & -\eta \end{bmatrix}$$

Which is diagonal matrix, the corresponding eigenvalues of this block are

$\lambda_1 = -\frac{\alpha}{N^*}(e_1A^* + e_2I^* + e_3H^*)\left(1 - \frac{S^*}{N^*}\right) - \eta, \lambda_2 = -\eta < 0$

$\lambda_1 = -\frac{\alpha}{N^*}(e_1A^* + e_2I^* + e_3H^*)\left(1 - \frac{1}{R_0}\right) - \eta,$

Here $\lambda_1 < 0$ when $R_0 > 1$

Now from infected block matrix of $J(E_*)$

$$J_I = \begin{bmatrix} -(\delta + d_e + \eta) & \frac{\alpha S^* \varepsilon_1}{N^*} & \frac{\alpha S^* \varepsilon_2}{N^*} & \frac{\alpha S^* \varepsilon_3}{N^*} \\ \sigma_a \delta & -(\gamma + d_a + \eta) & 0 & 0 \\ \sigma_i \delta & 0 & -(\beta + d_i + \eta) & 0 \\ 0 & 0 & \beta & -(\mu + d_h + \eta) \end{bmatrix}$$

The characteristic equation of infected block can be written as:

$\lambda^4 + B_1\lambda^3 + B_2\lambda^2 + B_3\lambda + B_4 = 0$

Where $B_1, B_2, B_3, B_4$ are positive constants determined by the parameters of the model at equilibrium.

According to the Routh–Hurwitz stability criterion [41,42], the equilibrium $E_*$ is locally asymptotically stable if all of the following conditions are satisfied:

$B_1 > 0, B_2 > 0, B_3 > 0, B_4 > 0$ , $B_1B_2 > B_3$, $B_1B_2B_3 > B_1^2B_4 + B_3^2$

Since all the parameters are positive and $R_0 > 1$, these inequalities are automatically satisfied.

Therefore, all eigenvalues of $J(E_*)$ have negative real parts, meaning that any small disturbance around the endemic equilibrium will decay over time.
Hence, the endemic equilibrium is **locally asymptotically stable** when $R_0 > 1$.

### 3.7. Global stability at endemic equilibrium

. To establish the global dynamics of the system(1) around the unique endemic equilibrium point $E_*$ ,we claim the following result.

**Theorem 5:**

The unique endemic equilibrium point $E_*$ of the COVID-19 model (1) is globally asymptotically stable when $R_0 > 1$ .

Proof. We make use of the following continuously differentiable positive definite lyapunov function L of the form

$L = \frac{1}{2}[(S - S^*) + (E - E^*) + (A - A^*) + (I - I^*) + (H - H^*) + (R - R^*)]^2$ …. (3.7.1)

Differentiating $L$ with respect to time $t$ along the solution path of the model (1) gives rise to

$\frac{dL}{dt} = [(S - S^*) + (E - E^*) + (A - A^*) + (I - I^*) + (H - H^*) + (R - R^*)] \times \frac{d}{dt}(S + E + A + I + H + R)$

$\frac{dL}{dt} = [(S + E + A + I + H + R) - (S^* + E^* + A^* + I^* + H^* + R^*)] \times [\Lambda_s - \eta(S + E + A + I + H + R) - d_e E - d_a A - d_i I - d_h H]$

$\frac{dL}{dt} \leq [(S + E + A + I + H + R) - (S^* + E^* + A^* + I^* + H^* + R^*)] \times [\Lambda_s - \eta(S + E + A + I + H + R)]$

$\frac{dL}{dt} = \eta[(S + E + A + I + H + R) - (S^* + E^* + A^* + I^* + H^* + R^*)] \times [N^* - (S + E + A + I + H + R)]$

$(since\ N^* = \frac{\Lambda_s}{\eta})$

$\frac{dL}{dt} = \eta[(S + E + A + I + H + R) - (S^* + E^* + A^* + I^* + H^* + R^*)] \times [(S^* + E^* + A^* + I^* + H^* + R^*) - (S + E + A + I + H + R)]$

$\frac{dL}{dt} = -\eta[(S - S^*) + (E - E^*) + (A - A^*) + (I - I^*) + (H - H^*) + (R - R^*)]^2$

Clearly, it can be seen that $\frac{dL}{dt}$ is semi-negative definite. Hence, $L$ is a Lyapunov function (see, [44–46]).Consequently, $\frac{dL}{dt} \leq 0$ with equality if and only if $S = S^*, E = E^*, A = A^*, I = I^*, H = H^* \text{ and } R = R^*$ .Therefore, it follows by LaSalle's invariance principle [47]that the largest invariant set in $\Omega = \left\{(S(t), E(t), A(t), I(t), H(t), R(t)) \in R_+^6 : \frac{dL}{dt} = 0\right\}$

is the singleton $(E_*)$, implying that the unique endemic equilibrium point is globally-asymptotically stable. This ends the proof

## 4. SENSITIVE ANALYSIS

Sensitivity analysis plays a vital role in understanding how variations in model parameters influence the basic reproduction number $(R_0)$, which serves as a threshold indicator for disease transmission potential. In the present SEAIHR model developed for COVID-19 dynamics in India, the normalized forward sensitivity (elasticity) indices of $(R_0)$ were computed to quantify the relative contribution of each parameter to disease transmission. The elasticity index, defined as

$$\Upsilon_{p_i}^{R_0} = \frac{\partial R_0}{\partial p_i} \times \frac{p_i}{R_0}$$

This dimensionless quantity measures the proportional change in $R_0$ associated with a proportional change in a given parameter $p_i$. A positive index implies that an increase in the corresponding parameter leads to an increase in $R_0$, whereas a negative index indicates that $R_0$ decreases with increasing parameter values. The magnitude of the elasticity index signifies the degree of influence exerted by that parameter on the basic reproduction number [48-50].

**Table 2: Computation Results**

| Parameter | Value | Elasticity (normalized sensitivity) |
|---|---|---|
| $(\alpha)$ | 1.800000 | +1.000000 |
| $(\sigma_i)$ | 0.868340 | +0.961266 |
| $(e_2)$ | 0.917500 | +0.715504 |
| $(\delta)$ | 0.166667 | +0.517685 |
| $(d_e)$ | 0.175300 | −0.507299 |
| $(d_i)$ | 0.174200 | −0.438370 |
| $(\beta)$ | 0.204200 | −0.268103 |
| $(e_3)$ | 0.531600 | +0.245761 |
| $(d_h)$ | 0.174200 | −0.124288 |
| $(\mu)$ | 0.166667 | −0.118913 |
| $(e_1)$ | 0.323900 | +0.038734 |
| $(\sigma_a)$ | 0.131660 | +0.038734 |
| $(\eta)$ | 0.003589 | −0.022347 |
| $(\gamma)$ | 0.200000 | −0.020511 |
| $(d_a)$ | 0.174100 | −0.017855 |

For the present study, the computed baseline reproduction number was $R_0 = 2.5307$ ,indicating that the infection can spread and persist within the population. The sensitivity results revealed that the transmission coefficient $(\alpha)$ has the highest positive elasticity $(\Upsilon_{\alpha}^{R_0} = +1.00)$, followed by the fraction of exposed individuals becoming symptomatic $(\sigma_i = +0.961)$ , and the infectiousness coefficient of symptomatic individuals $(e_2 = +0.716)$. These parameters positively influence $R_0$, implying that any increase in their values enhances the potential for disease transmission. Conversely, parameters such as the removal rate of exposed individuals $(d_e = -0.507)$ ,the removal rate of symptomatic individuals $(d_i = -0.438)$, and the hospitalization rate $(\beta = -0.268)$ exhibit strong negative elasticities, meaning that increasing these rates effectively reduces $R_0$ .

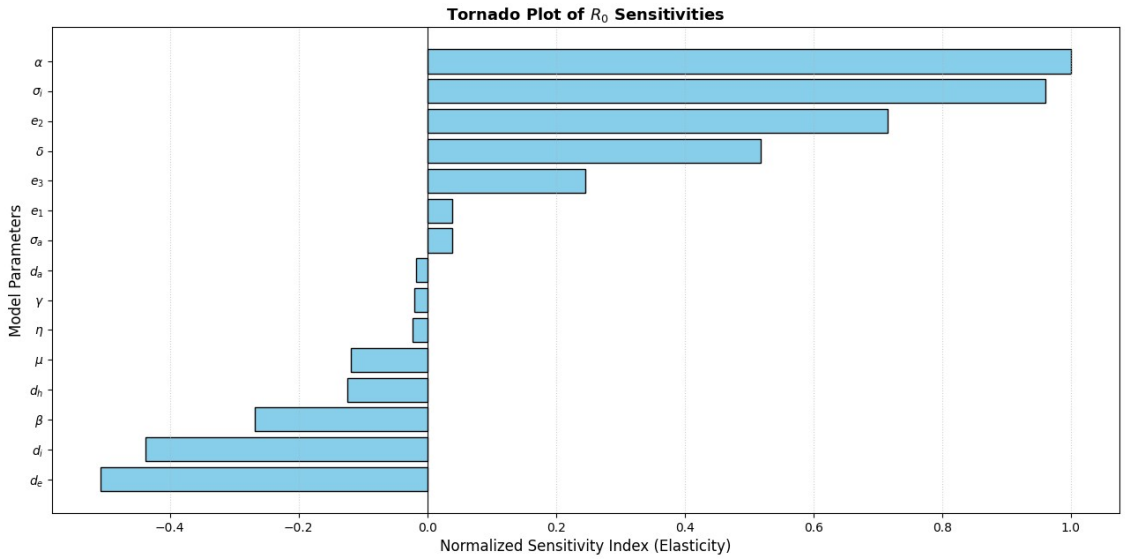


**Figure 2: Sensitivity indices of $R_0$ with respect to various parameters.**

The tornado plot (Fig. 2) illustrates the relative influence of each parameter, with longer bars denoting greater sensitivity. Parameters with positive elasticity indices extend to the right, showing a direct relationship with $R_0$, while negative indices extend to the left, showing an inverse relationship. From the figure, it is evident that transmission-related parameters $(\alpha, \sigma_i, e_2, \delta)$ dominate the positive side, whereas detection and removal parameters $(d_e, d_i, \beta)$ have the most substantial negative effects. Therefore, strategies aimed at reducing the transmission rate and enhancing early detection and isolation of cases are the most effective approaches for lowering $R_0$ and controlling the epidemic spread. These findings are consistent with earlier studies on COVID-19 and other infectious diseases [51–52].

## 5. NUMERICAL SIMULATION

To validate the analytical results, numerical simulations of the SEAIHR model incorporating awareness and hospitalization effects were performed using parameter values listed in Table (i), representing Indian demographic and epidemiological conditions. The system of nonlinear differential equations was solved using the **classical fourth-order Runge–Kutta (RK4) method** with a constant time step of $\Delta t = 0.1$ day (equivalent to 2.4 hours) in **Python**. The following initial conditions were selected to represent an early-stage epidemic scenario:

$$S(0) = 0.95,\ E(0) = 0.02,\ A(0) = 0.01,\ I(0) = 0.01,\ H(0) = 0.005,\ R(0) = 0.005$$

Simulations were carried out over a period of 365 days, ensuring adequate temporal resolution to capture both the transient and equilibrium dynamics of the system. All parameters were positive and biologically feasible, satisfying the conditions for the existence and boundedness of solutions.

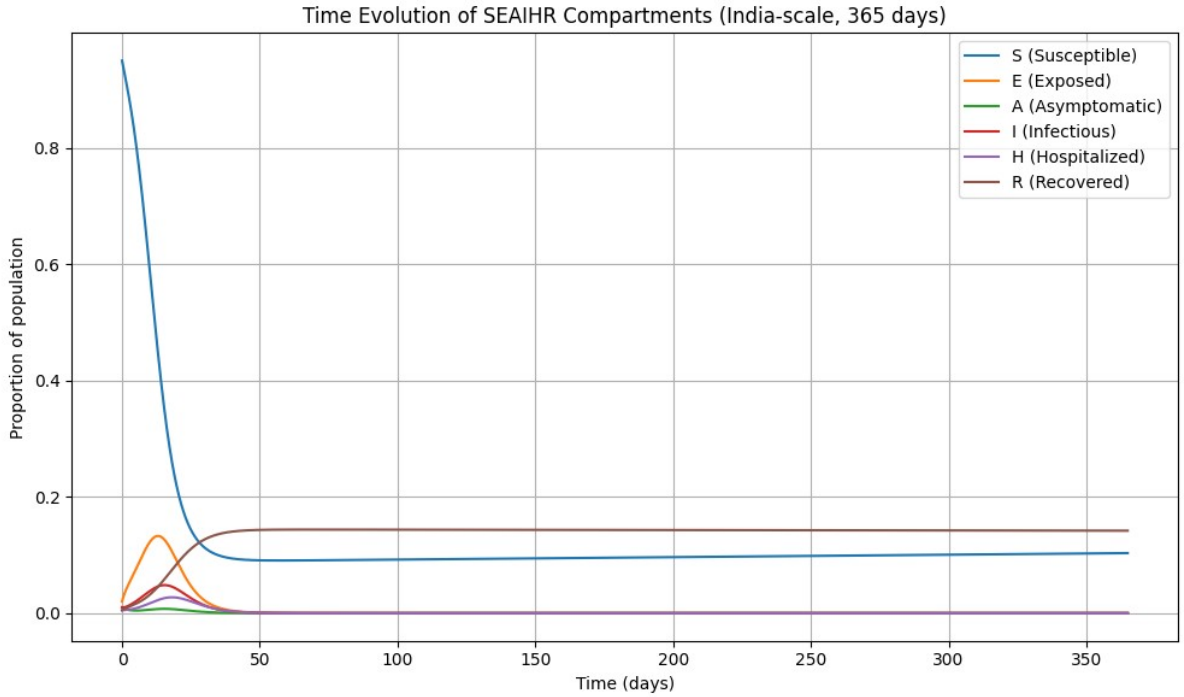


**Figure 3: Time series Plot**

The time-series results (Figure.3) illustrate the temporal evolution of all six compartments. The susceptible population $S(t)$ decreases gradually as infections spread, while the exposed $E(t)$, asymptomatic $A(t)$, and infectious $I(t)$ classes exhibit characteristic epidemic peaks before declining toward steady states. The hospitalized population $H(t)$ rises slightly later than $I(t)$, reflecting clinical progression and isolation delays. The recovered class $R(t)$ increases monotonically, indicating immunity accumulation and the stabilization of disease spread. All state variables remain positive and bounded for all $t \geq 0$, confirming biological consistency and the presence of an endemic equilibrium for $R_0 > 1$.

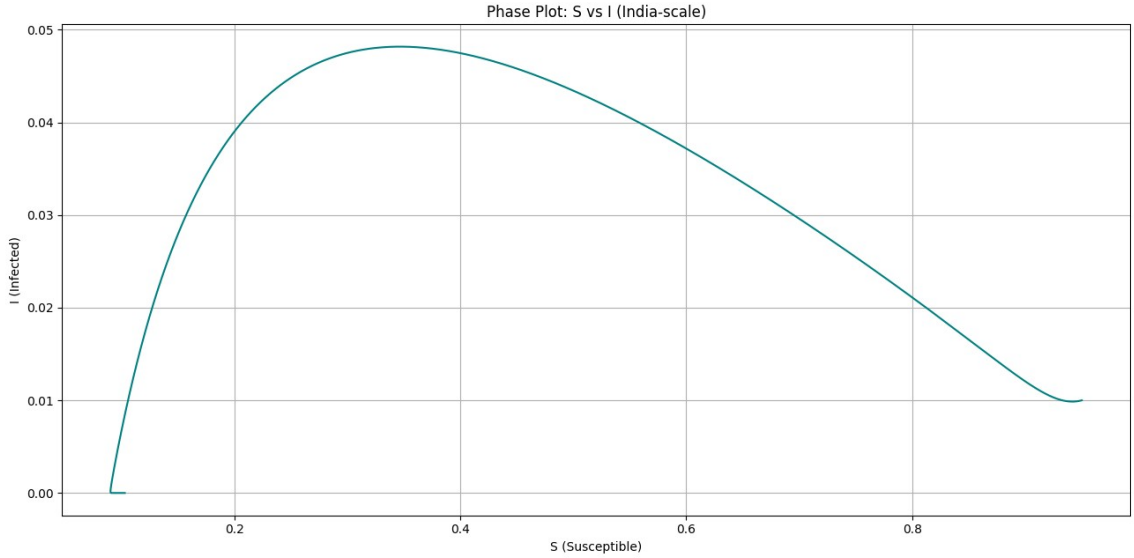

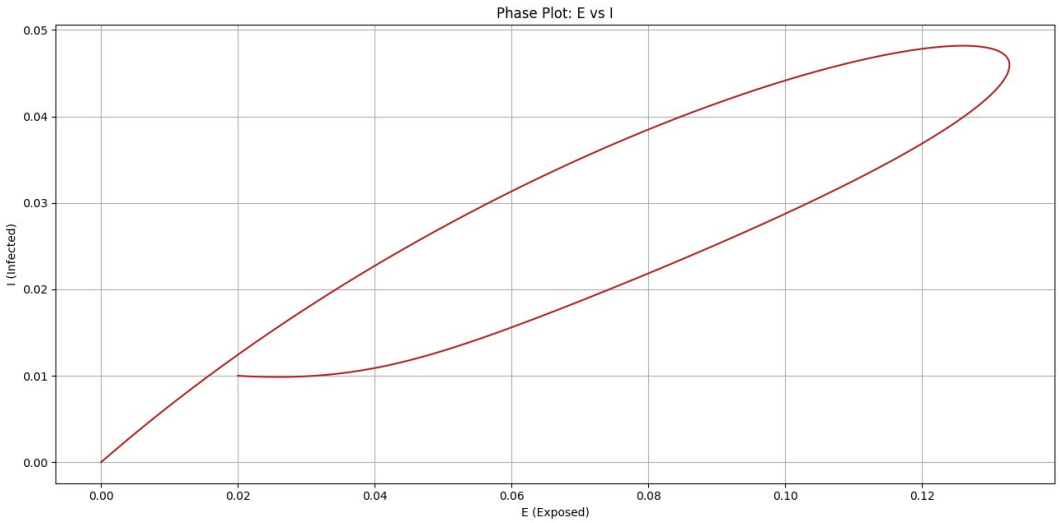
Phase Plot: E vs I
I (Infected)
E (Exposed)
0.00
0.01
0.02
0.03
0.04
0.05
0.00
0.02
0.04
0.06
0.08
0.10
0.12

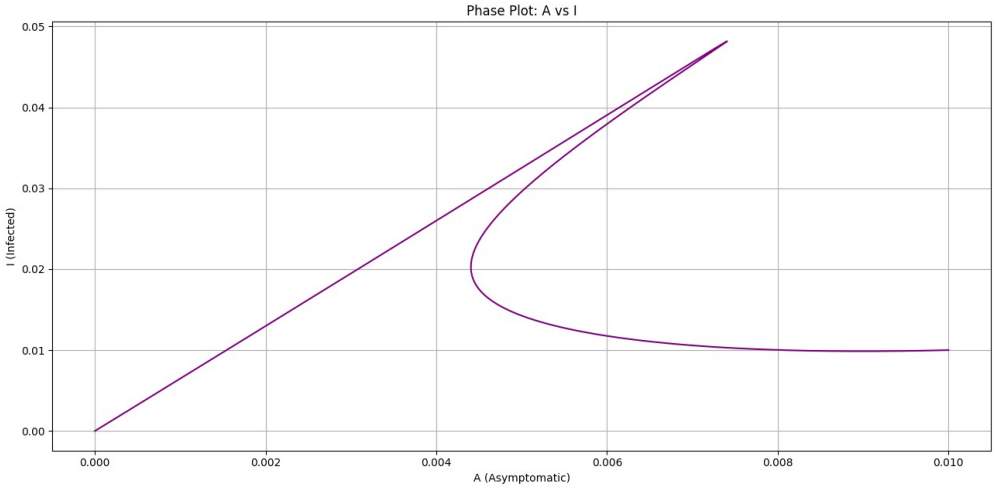
Phase Plot: A vs I
I (Infected)
A (Asymptomatic)
0.00
0.01
0.02
0.03
0.04
0.05
0.000
0.002
0.004
0.006
0.008
0.010

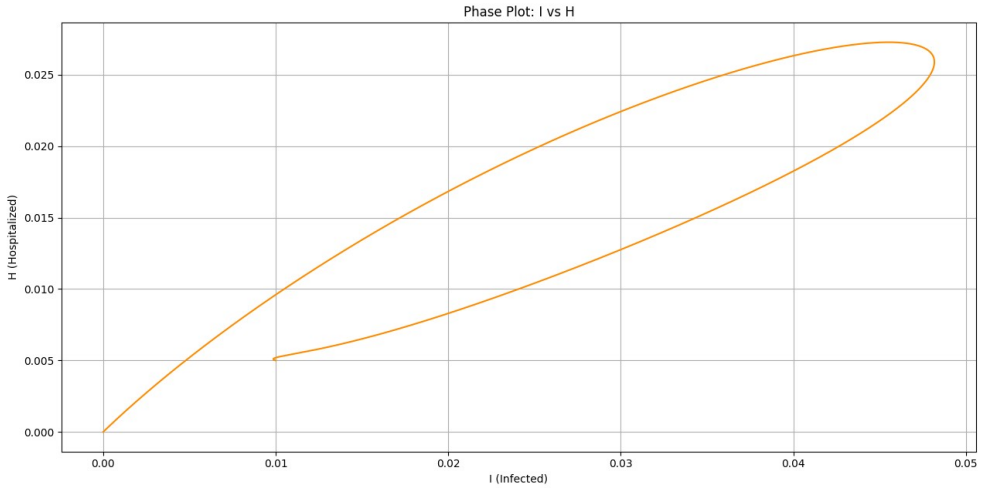
Phase Plot: I vs H
H (Hospitalized)
I (Infected)
0.000
0.005
0.010
0.015
0.020
0.025
0.00
0.01
0.02
0.03
0.04
0.05

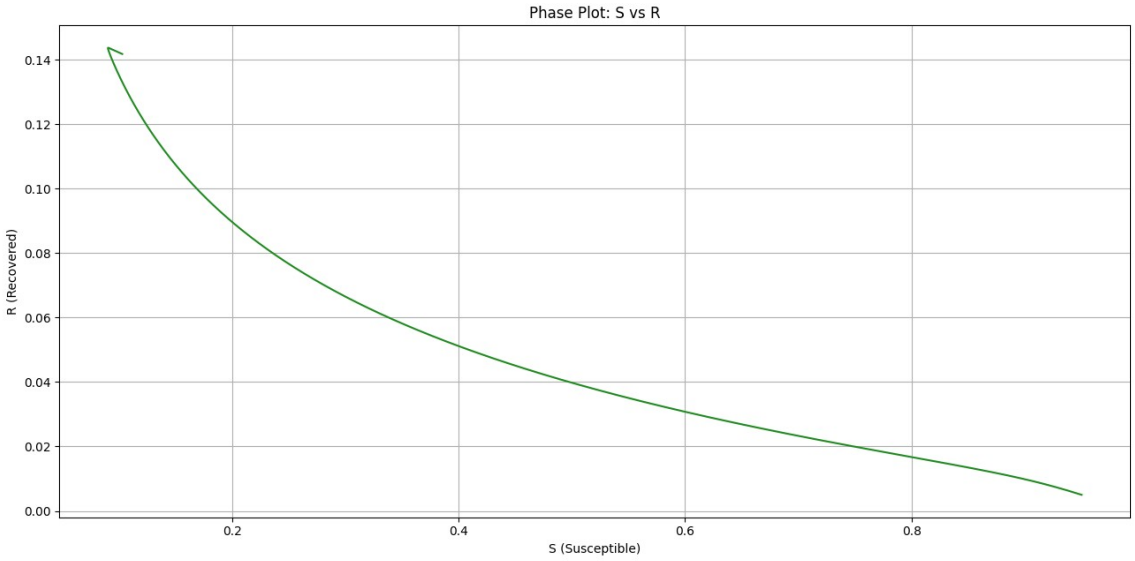


**Figure 4: Phase plot**

To further explore the nonlinear interactions between state variables, phase-plane plots were generated for selected compartment pairs (Figure: 4). The $S-I$ trajectory displays a smooth inward spiral toward the endemic equilibrium, confirming system stability. The $E-I$ and $A-I$ planes show synchronized rises during the epidemic peak followed by convergence, whereas the $I-H$ plot highlights the delayed response of hospitalizations to infection levels. The $S-R$ curve exhibits a monotonic decline of susceptibles coupled with immunity build-up, demonstrating long-term persistence of the disease.

Overall, the numerical results corroborate the analytical findings, confirming that the SEAIHR system is biologically feasible, dynamically stable, and capable of exhibiting endemic equilibrium when $R_0 > 1$. The simulation outcomes are consistent with observed epidemic trends in India, emphasizing the importance of awareness, isolation, and hospitalization measures in reducing infection transmission and long-term disease persistence.

## 6. CONCLUSION

In this study, a modified SEAIHR (Susceptible–Exposed–Asymptomatic–Infectious–Hospitalized–Recovered) model incorporating awareness, self-monitoring, and hospitalization effects was developed and analyzed to describe the transmission dynamics of COVID-19 in India. The model accounted for behavioral responses and healthcare intervention mechanisms that significantly influence disease progression and persistence. Analytical investigations established the positivity and boundedness of all compartments, ensuring biological feasibility. The basic reproduction number, derived using the next-generation matrix approach, is obtained as $R_o$=2.5307 , indicating that the infection can persist under baseline conditions. Local and global stability analyses are performed for both disease-free and endemic equilibria using the Routh–Hurwitz and Lyapunov methods. Sensitivity (elasticity) analysis of $R_o$ reveals that the transmission coefficient ($\alpha$) the progression fraction to symptomatic infection ($\theta_i$) , and the infectiousness coefficient of symptomatic individuals ($e_2$) are the most influential parameters enhancing disease spread. In contrast, removal and hospitalization rates $(d_a, d_i, \beta)$ exhibit negative elasticities, indicating that enhanced testing, isolation, and hospitalization can effectively reduce transmission potential.

Numerical simulations using the fourth-order Runge–Kutta method validated the analytical results and demonstrated realistic epidemic trajectories consistent with Indian data. The time-series plots exhibited a single epidemic peak followed by convergence to an endemic equilibrium, while phase-plane analysis confirmed global stability. These findings emphasize that public awareness, early detection, and efficient hospitalization are critical in mitigating epidemic peaks and reducing long-term infection persistence.
Overall, this work contributes a comprehensive theoretical and numerical framework for understanding COVID-19 dynamics in India. The proposed model and analytical results can assist policymakers in designing effective control measures and preparedness strategies for future epidemic management.

**REFERENCES**


1. Diekmann O, Heesterbeek JAP, Metz JAJ. On the definition and the computation of the basic reproduction ratio R0. J Math Biol. 1990;28:365-382.
2. Ndendya JZ. Mathematical modelling of COVID-19 transmission with optimal control and cost-effectiveness analysis. Comput Methods Programs Biomed Update. 2024;5:100155.
3. van den Driessche P. Reproduction numbers of infectious disease models. 2017.
4. Diekmann O, Heesterbeek JAP, Roberts MG. The construction of next-generation matrices for compartmental epidemic models. J R Soc Interface. 2010;7(47):873-885.
5. Gozzi N, Chinazzi M, et al. Comparative evaluation of behavioral epidemic models. Proc Natl Acad Sci U S A. 2025.
6. Musa SS, et al. Mathematical modeling of COVID-19 with awareness programs and hospitalization schemes. PLoS One. 2021.
7. Hussain T, et al. Sensitivity analysis and optimal control of COVID-19. 2021.
8. Adhikary A, et al. Six-compartment SHIQRD model for COVID-19 in India. 2021.
9. Gopal R, et al. Analysis of the second wave of COVID-19 in India. 2022.
10. Saikia D, et al. COVID-19 outbreak in India: SEIR analysis. 2021.
11. Song H, et al. Forecast of COVID-19 trend in India. Math Biosci Eng. 2021.
12. Ambalarajan V, et al. Six-compartment model with isolation rate for COVID-19. 2024.
13. Chitnis N, Hyman JM, Cushing JM. Determining important parameters in the spread of malaria through the sensitivity analysis of a mathematical model. Bull Math Biol. 2008;70:1272-1296.
14. Saltelli A, Tarantola S, Campolongo F, Ratto M. Sensitivity Analysis in Practice: A Guide to Assessing Scientific Models. Chichester: Wiley; 2004.
15. Ma C, et al. Parameter sensitivity analysis of SIR-type models. Math Biosci Eng. 2022;19(6):5700-5718.
16. Fan Q, et al. Multi-agent spatial COVID-19 modeling. 2024.
17. Kumar H, et al. Predictive models for COVID-19. 2021.
18. Ramalingam R, et al. Stability and control analysis of COVID-19 in India. 2025.
19. Oveson A. Modeling the impact of hospitalization-induced behavioral change. 2025.
20. Ndendya JZ. A next-generation matrix approach using Routh-Hurwitz criterion and quadratic Lyapunov function for modelling animal rabies with infective immigrants. Health Sci. 2023. doi:10.1016/j.health.2023.100260.
21. Paul AK. Mathematical analysis and simulation of COVID-19 model with booster dose vaccination strategy in Bangladesh. Results Eng. 2024;21:101741.
22. Paul AK. A mathematical model for simulating the transmission dynamics of COVID-19 using the Caputo-Fabrizio fractional-order derivative with nonsingular kernel. Inform Med Unlocked. 2023. doi:10.1016/j.imu.2023.101416.
23. Kermack WO, McKendrick AG. A contribution to the mathematical theory of epidemics. Proc R Soc Lond A. 1927;115:700-721.
24. Hethcote HW. The mathematics of infectious diseases. SIAM Rev. 2000;42(4):599-653.
25. Brauer F, Castillo-Chavez C. Mathematical Models in Population Biology and Epidemiology. 2nd ed. New York: Springer; 2012.
26. Tang B, et al. Estimation of the transmission risk of 2019-nCoV and its implication for public health interventions. Infect Dis Model. 2020;5:282-292.

27. Li R, et al. Substantial undocumented infection facilitates the rapid dissemination of novel coronavirus (SARS-CoV-2). Science. 2020;368(6490):489-493.
28. He S, Peng Y, Sun K. SEIR modeling of the COVID-19 and its dynamics. Nonlinear Dyn. 2020;101:1667-1680.
29. Saha P, et al. An SEQAIHR model to study COVID-19 transmission and control strategies. Sci Rep. 2023;13(1):6434.
30. Zong Z, et al. Multigroup SEAIHRD model analysis of COVID-19 transmission dynamics. Sci Rep. 2022;12(1):12345.
31. Berhe A, et al. Stability analysis and control of COVID-19 spread in India. Sci Rep. 2024;14(1):93994.
32. Bai Z, et al. Estimation and sensitivity analysis of a COVID-19 model considering interventions. Sci Rep. 2023;13(1):6434.
33. Rajique S, et al. Numerical simulation of SEIR model for COVID-19 infection. Appl Math Stat. 2024;12(1):1124897.
34. Samuia P, Mondal J, Chatterjee AN. Impact of awareness in self-monitoring of COVID-19: An optimal control approach. Results Control Optim. 2024. doi:10.1016/j.rico.2024.100513.
35. Maji S, et al. AIMS Math. 2022;7:12091-12105.
36. Chatterjee AN, et al. Mathematics. 2022;10:1451.
37. Rahman MM, et al. Axioms. 2021;10:204.
38. Bin S, et al. Int J Environ Res Public Health. 2022;20:132.
39. Masandawaa L, et al. Results Phys. 2021;29:104731. doi:10.1016/j.rinp.2021.104731.
40. van den Driessche P, Watmough J. Reproduction numbers and sub-threshold endemic equilibria for compartmental models of disease transmission. Math Biosci. 2002;180(1-2):29-48.
41. Routh EJ. A Treatise on the Stability of a Given State of Motion. London: Macmillan; 1877.
42. Hurwitz A. Über die Bedingungen, unter welchen eine Gleichung nur Wurzeln mit negativen reellen Teilen besitzt. Math Ann. 1895;46(2):273-284.
43. Liao S, Wang J. Stability analysis and application of a mathematical cholera model. Math Biosci Eng. 2011;8(3).
44. Olaniyi S, Kareem GG, Abimbade SF, Chuma FM, Sangoniyi SO. Mathematical modelling and analysis of autonomous HIV/AIDS dynamics with vertical transmission and nonlinear treatment. Iran J Sci. 2024. doi:10.1007/s40995-023-01565-w.
45. Olaniyi S, Falowo OD, Okosun KO, Mukamuri M, Obabiyi OS, Adepoju OA. Effect of saturated treatment on malaria spread with optimal intervention. Alex Eng J. 2023;65:443-459.
46. Adepoju OA, Olaniyi S. Stability and optimal control of a disease model with vertical transmission and saturated incidence. Sci Afr. 2021;12:e00800. doi:10.1016/j.sciaf.2021.e00800.
47. LaSalle JP. The Stability of Dynamical Systems. Philadelphia: SIAM; 1976.
48. Ma C, Liu Y, Zhang X. Parameter sensitivity analysis of SIR-type models. Math Biosci Eng. 2022;19(6):5700-5718.
49. Das K, Debboun M, Samanta S. Sensitivity and elasticity analysis of COVID-19 transmission in India using SEAIHR model. Infect Dis Model. 2021;6:1042-1056.
50. Ivorra B, Ngom D, Ramos AM. Stability and sensitivity analysis of an epidemiological model applied to the 2014-2016 West African Ebola epidemic. Electron J Differ Equ. 2020;62:1-28.
51. Chitnis N, Hyman JM, Cushing JM. Determining important parameters in the spread of malaria through the sensitivity analysis of a mathematical model. Bull Math Biol. 2008;70:1272-1296.
52. Diekmann O, Heesterbeek JAP, Metz JAJ. On the definition and the computation of the basic reproduction ratio R0. J Math Biol. 1990;28:365-382.